Simplified stability analysis of quasi-brittle notched columns

L. Fenu
Department of Structural Engineering, University of Cagliari, Italy

ABSTRACT: The stability of columns made of quasi-brittle materials, loaded by an eccentric force at the top and edge notched at their base, is studied. Actually, columns are often made of quasi-brittle materials, as it happens for stone columns of historical monuments. They are frequently cracked or notched at the base, as this region is both more solicited and exposed to impacts that can chip them. Besides, columns are often slender, so that geometrical instability can also occur. Therefore, simplified methods of analyzing the instability due to both column geometry and fracture are useful, as the both can occur contemporarily. A simplified analysis of the instability of notched slender columns is then illustrated, by also avoiding the use of finite elements. This appears to be an advantage, because an easy analysis, although approximated, allows a faster check of the column stability, as well as an intuitive comprehension.

1 INTRODUCTION

Columns are often made of quasi-brittle materials, for instance natural conglomerates like sandstones and limestones, and artificial conglomerates like mortars and concretes. The example of stone columns of historical monuments is well known.

Their static duty is to transmit compression forces, but bending can also occur so that tensile stresses can arise. Resistance can then be checked through the interaction diagram of axial load versus bending moment; if the column is not too slender and without damages, only this check is needed.

Unfortunately, sometimes columns are also quite slender, so that geometric instability has to be taken into account. Besides, they are often notched, for instance accidentally chipped by an impact - as it often happens in old stone columns of many monuments - as well as cracked and damaged. Therefore, they can be subjected to both geometric and fracture instability.

If the column is enough slender, the interaction diagram has to be restrained by taking into account the geometric stability of the column itself depending on its slenderness.

A general approach to the geometric instability of columns has to take into account both the second order effects and the mechanical non-linearity of the material. A nonlinear Finite Element Analysis is usually required, and the support of computer-aided computations is usually necessary (Bazant & Cedolin 1991). Therefore, simplified methods are also used, as, in many cases, sufficiently approximated results can be obtained. Besides, an easy analysis of column instability is often useful. Among the different methods of analysing the column stability in order to restrain the interaction diagram, a simplified analysis can be run by using the Model Column Method. Its use can be really advantageous, provided the moment-curvature diagrams are easily available: a simple method of achieving them for every normal compression force of the interaction diagram is described, so allowing us to easily use the Model Column Method.

Besides, columns are often notched, as well as cracked or damaged. Although columns are usually compressed, an excessive eccentricity of the compression force makes tensile stresses arise close to the notch region or the damaged zone, so that fracture can become instable, and also propagate catastrophically in spite of significant compressive forces transmitted to the column base. The interaction diagram can then be restrained due to not only column geometric instability, but also to fracture instability depending on the notch depth. For sake of simplicity, in the following we consider the case of rectangular columns loaded at the top by an eccentric vertical force and with a horizontal edge notch at their base.

The fracture behaviour of quasi-brittle materials deviates significantly from linearity due to the microcracks in the fracture process zone ahead of the notch. Appropriate nonlinear theories have been developed to model this nonlinear behaviour. Suitable

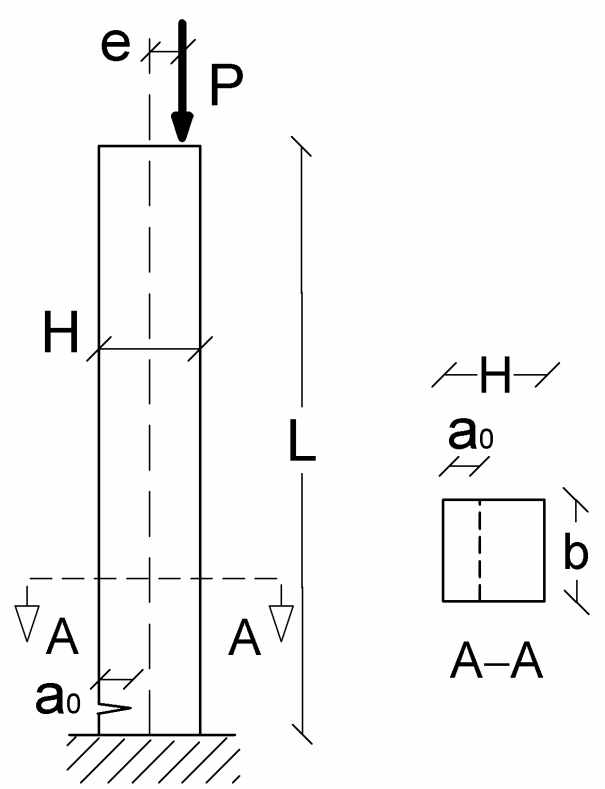

Figure 1. Scheme of the eccentrically loaded column with an edge notch at its base.

nonlinear crack models are the Fictitious Crack Model (Hillerborg et al. 1976, Nallathambi & Karihaloo 1986) and the Crack Band Model (Bazant 1976, Bazant & Cedolin 1979, Bazant & Oh 1983), but in general they have to be implemented with a Finite Element Algorithm. Since in this paper a simplified analysis is required, besides geometric instability, also fracture instability is analysed through a simplified model. Through Bazant's Size Effect Model (Bazant 1984, Bazant 1987), we then construct a so-called *R*-curve, or resistance curve, in a parametric form (Bazant & Kazemi, 1990).

By then considering the above notched column, through the *R*-curve we analyse the fracture stability for every compression force of the interaction diagram as well as for different eccentricities and notch depths. In this way we can approximate the nonlinear fracture behaviour of the quasi-brittle material through the well known relations of Linear Elastic Fracture Mechanics, allowing us a simplified analysis of the stability of notched columns to finally achieve an interaction diagram restrained by both geometric and fracture instability.

2 CONSTRUCTION OF THE THE INTERACTION DIAGRAM OF AXIAL LOAD VERSUS BENDING MOMENT

We assume that the behaviour of the quasi-brittle material in compression is represented by a parabolic stress-strain relationship up to a strain ε_{c0}, from which point onward the strain increases up to an ultimate strain ε_{cu} while the stress remains at the constant value $0.85\,f_c$, where f_c is the cylindrical compressive strength of the quasi-brittle material. For f_{ct} being its tensile strength, we also assume that the behaviour in tension is represented by a parabolic stress-strain relationship up to a point with strain ε_{t0}, where the collapse is reached. Although the strains ε_{c0}, ε_{cu}, ε_{t0} depend on the mechanical characteristics of the quasi-brittle material, like strength for instance, in this paper their values are assumed to be ε_{c0}=0.002, ε_{cu}=0.0035, ε_{t0}=0.00015 respectively, that are suitable values for a number of cases.

Consider a column whose cross section has depth H and breadth b. For x being the depth of the neutral axis, its adimensional value is $\xi=x/H$; at ultimate, it is assumed to be $\xi_u=x_u/H$ By assuming that plane sections remain plane till the collapse, failure can occur with or the neutral axis intersecting the column or being outside. In the first case it is reached when or the maximum compressive strain is ε_{cu}, or the maximum tensile strain is ε_{t0}; both strains can also be reached contemporarily, for $\xi_u=1/(1+|\varepsilon_{t0}/\varepsilon_{cu}|)$, that is for ξ_u=0.9589. In all these cases the eccentricity is greater than $H/6$. Otherwise, when it is smaller than $H/6$, failure occurs for $\xi_u>1$, and, analogously to the well known case of reinforced concrete sections, all the linear strain diagrams at ultimate pass on the point identified by the intersection of the line of constant compressive strain ε_{c0} and that of the strain diagram for ξ_u=1.

It is worth using the stress-block for both compressive and tensile stresses, defined by the length of their sides and by the position of their stress resultant.

Let us assume that for compressions its horizontal side is $0.85\,f_c$. Assuming Sargin's law as stress-strain relationship (Sargin, 1971), by knowing the strains along the section the related stress distribution is also known.

By integrating it at ultimate, its resultant force is put equal to $R_{cu}(\xi_u)=0.85\,f_c b\beta_{1c}(\xi_u)x_u$, with $\beta_{1c}(\xi_u)x_u$ assumed to be the stress-block vertical side; $\beta_{1c}(\xi_u)$ is a function of ξ_u, as, at ultimate, each ξ_u corresponds to a specific strain ε_e of the compressed edge. Therefore, the vertical side of the stress-block can also be written as $\beta_{1c}(\varepsilon_e)x_u$. From the previous integration, by evaluating the centroid of the compressive stresses, the position of the stress resultant at ultimate is also obtained, that is its distance $\beta_{2c}(\xi_u)x_u$ from the compressed edge, as well as its distance $d_c(\xi_u)=H/2-\beta_{2c}(\xi_u)x_u$ from the section centroid. Also $\beta_{2c}(\xi_u)$ is a function of ξ_u, and, analogously to the case of function β_{1c}, it can be assumed that $d_c(\varepsilon_e)=H/2-\beta_{2c}(\varepsilon_e)x_u$.

The stress block of tensile stresses can be described analogously. Let us assume that also for tensile stresses with $0\leqslant\varepsilon\leqslant\varepsilon_{t0}$ the parabolic stress-strain relationship follows Sargin's law; besides, the hori-

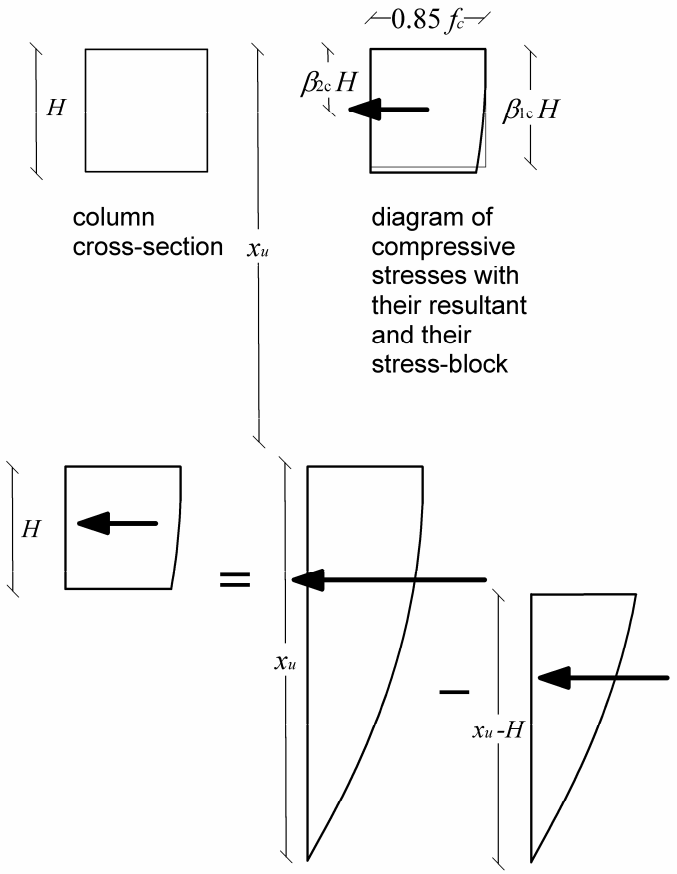

Figure 2. Diagram of the column compressive stresses for x_u>H obtained by means of subtraction, and their stress-block.

zontal side of the stress-block is assumed to be f_{ct}. Since at ultimate each value of tensile strain ε_i at the edge in tension corresponds to a value (1-ξ_u), the vertical side of the stress-block is assumed to be $\beta_{1t}(1-\xi_u)\cdot(H-x_u)$, with β_{1t} as a function of ξ_u. This side length is obtained by integrating the relationship between strain and tensile stresses and by then imposing that its integral at ultimate is $R_{tu}(\xi_u)=f_{ct}b\beta_{1t}(1-\xi_u)\cdot(H-x_u)$. To evaluate the position of R_{tu}, its distance from the edge in tension and from the section centroid is assumed to be $\beta_{2t}(1-\xi_u)\cdot(H-x_u)$ and $d_t(\xi_u)=H/2-\beta_{2t}(\xi_u)\cdot(H-x_u)$ respectively, with also $\beta_{2t}(\xi_u)\cdot$as a function of ξ_u. Analogously to the case of compressions, R_{tu} and $d_t(\xi_u)$ can also be put as $f_{ct}\cdot\beta_{1t}(\varepsilon_i)\cdot(H-x_u)$ and $H/2-\beta_{2t}(\varepsilon_i)\cdot(H-x_u)$, respectively.

When ξ_u>1 and the whole section is compressed; by referring to Figure 2, if the strain of the most compressed edge is ε_e and that of the less compressed one is ε_i, we have (Biasioli et al):

$$\beta_{1c}(\xi_u)=\beta_{1c}(\varepsilon_e)\cdot\xi_u-\beta_{1c}(\varepsilon_i)\cdot(\xi_u-1) \tag{1a}$$

$$\beta_{2c}(\xi_u)=\frac{[\beta_{2c}(\varepsilon_e)\cdot\xi_u][\beta_{1c}(\varepsilon_e)\cdot\xi_u]}{\beta_{1c}(\xi_u)}- +\frac{[\beta_{2c}(\varepsilon_i)\cdot(\xi_u-1)+1][\beta_{1c}(\varepsilon_i)\cdot(\xi_u-1)]}{\beta_{1c}(\xi_u)} \tag{1b}$$

with $\varepsilon_i=\varepsilon_e\cdot(\xi_u-1)/\xi_u$. The compressive stress resultant and its position with respect to the section centroid are $R_{cu}(\xi_u)=0.85\,f_c\,b\beta_{1c}(\xi_u)H$ and $d_c(\xi_u)=H/2-\beta_{2c}(\xi_u)H$, respectively.

By then considering both the equilibrium equation in the column axis direction and the moment equilibrium for $0\leqslant\xi_u\leqslant+\infty$, the axial load $N_u(\xi_u)$ and the bending moment $M_u(\xi_u)$ at ultimate are then obtained. For $0\leqslant\xi_u<1$ the ultimate axial load is $N_u(\xi_u)=R_{cu}(\xi_u)-R_{tu}(\xi_u)$, while the ultimate moment is $M_u(\xi_u)=R_{cu}(\xi_u)\cdot d_c(\xi_u)+R_{tu}(\xi_u)\cdot d_t(\xi_u)$; for ξ_u>1 they become $N_u(\xi_u)=R_{cu}(\xi_u)$ and $M_u(\xi_u)=R_{cu}(\xi_u)\cdot d_c(\xi_u)$.

The interaction diagram of axial load versus bending moment is therefore found.

Since in this paper the stability behaviour of columns is studied, tensile normal forces are not considered, and the interaction diagram is then restrained to only compressive forces $N_u(\xi_u)$. In the following, the interaction diagram will be further restrained by both geometric and fracture instability.

3 USE OF THE MODEL COLUMN METHOD

Although approximate, the Model Column Method is diffusely used in structural engineering. Its main simplifications consist in assigning the trend of the second order displacements along the column and in localising the analysis of the equilibrium stability only at the column base. Nevertheless, the method is included in a number of codes, and by investigating a simplified analysis of the column stability, it is therefore worth using it.

3.1 *Construction of the moment-curvature diagrams*

Moment-curvature diagrams depend on the section normal force. From a given couple (N, M) there are infinite paths to reach the collapse, but when columns are studied, if P is the axial load, it is worth investigating the path with constant normal force N, till $P = N_u$ for the ultimate moment M_u.

For every normal force P, it is achieved a different moment-curvature diagram. Consider a certain normal force P among the ones of the interaction diagram N-M: therefore there is a certain ξ_u so that $N_u(\xi_u)=P$. Consider for instance a normal force P applied along the column axis; unless secondary displacements occur, no moments arise along the column with concrete behaviour almost linear-elastic if P is small enough. By then increasing the eccentricity e, the whole column is subjected to the bending moment $M=P\cdot e$ that increases with e till, for this given ξ_u, an eccentricity e_u is reached, so that the collapse is also reached with $P\cdot e_u=M_u(\xi_u)$. Consider then $M=Pe$ small enough to have ξ>1. The translation equilibrium leads to $P=0.85f_cb\beta_{1c}H$. This equation is in general satisfied for different values of ξ, so that if ξ has to be found an edge strain has to be given, for instance ε_e, and viceversa; since all the

equation terms are given constants except β_{1c}, then β_{1c} is a function of both ξ and ε_e.

By increasing e the moment M increases, too, till the neutral axis intersects the cross section and $\xi<1$. In this case the translation equilibrium leads to:

$$P = 0.85 f_c b \beta_{1c} \xi H - f_{ct} b \beta_{1t} (1 - \xi H) \qquad (2)$$

For $\xi<1$ the resultants of compressive and tensile stress distributions have to match equation (2). Since these resultants depend on the strains ε_e and ε_i on the edge in compression and in tension respectively – related one another by the linear strain distribution – then ε_e and ξ cannot vary independently, and both functions β_{1c} and β_{1t} can depend on only an edge strain, for instance ε_e. Therefore, it can be put $\beta_{1c}=\beta_{1c}(\varepsilon_e)$ and $\beta_{1t}=\beta_{1t}(\varepsilon_i)$, but with $\varepsilon_i=\varepsilon_e\cdot(1-\xi)/\xi$, so that β_{1t} actually depend on ε_e in order to match the linear strain distribution along the section, as well as equation (2).

Therefore, when the collapse is not still reached, and ξ has not reached ξ_u, for $\xi\leq 1$ it can be put:

$$\beta_{1c}(\xi,\varepsilon_e) = \beta_{1c}(\varepsilon_e) \qquad (3a)$$

$$\beta_{2c}(\xi,\varepsilon_e) = \beta_{2c}(\varepsilon_e) \qquad (3b)$$

and, for $\xi>1$:

$$\beta_{1c}(\xi,\varepsilon_e) = \beta_{1c}(\varepsilon_e)\cdot\xi - \beta_{1c}\left(\varepsilon_e \frac{\xi-1}{\xi}\right)\cdot(\xi-1) \qquad (4a)$$

$$\beta_{2c}(\xi,\varepsilon_e) = \frac{\left(\beta_{2c}(\varepsilon_e)\cdot\xi\right)\cdot\left(\beta_{1c}(\varepsilon_e)\cdot\xi\right)}{\beta_{1c}(\xi,\varepsilon_e)} - \frac{\left[\beta_{2c}\left(\varepsilon_e \frac{\xi-1}{\xi}\right)\cdot(\xi-1)+1\right]\cdot\left[\beta_{1c}\left(\varepsilon_e \frac{\xi-1}{\xi}\right)\cdot(\xi-1)\right]}{\beta_{1c}(\xi,\varepsilon_e)} \qquad (4b)$$

The contour plot of the functions $\beta_{1c}=\beta_{1c}(\xi,\varepsilon_e)$ and $\beta_{2c}=\beta_{2c}(\xi,\varepsilon_e)$ is shown in Figures 3 and 4.

For $\xi>1$ functions β_{1t} and β_{2t} vanish, due to the absence of tensile stresses, so that they are only defined for $\xi\leq 1$, that is:

$$\beta_{1t}(\xi,\varepsilon_e) = \beta_{1t}(\varepsilon_e) \qquad (5a)$$

$$\beta_{2t}(\xi,\varepsilon_e) = \beta_{2t}(\varepsilon_e) \qquad (5b)$$

Let us now describe the moment-curvature diagram for a certain axial force $N_u(\xi_u)=P$ among the ones available in the interaction diagram M-N. For P=cost the translation equilibrium is:

$$N_u(\xi_u) = R_c(\xi,\varepsilon_e) - R_t(\xi,\varepsilon_e) \qquad (6)$$

with:

$$R_c(\xi,\varepsilon_e) = 0.85 f_c b \beta_{1c}(\xi,\varepsilon_e)\cdot\xi H \qquad (7a)$$

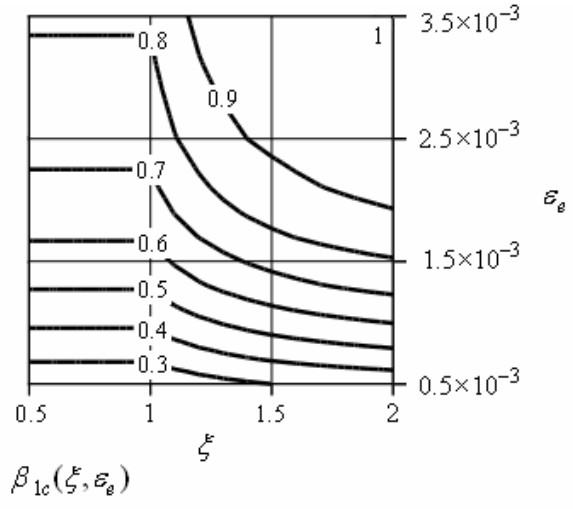

Figure 3. Contour plot of the function $\beta_{1c}=\beta_{1c}(\xi,\varepsilon_e)$.

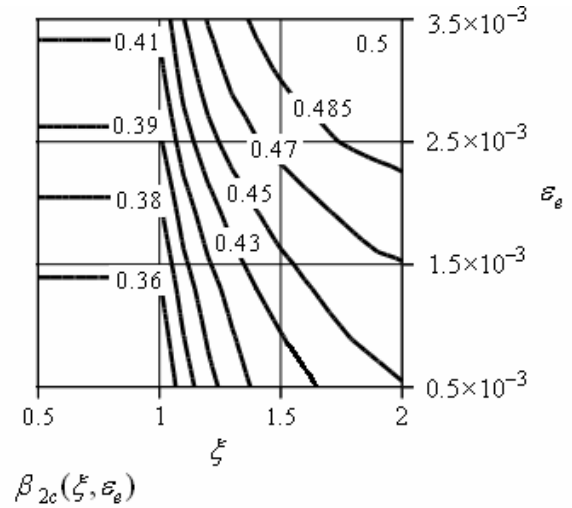

Figure 4. Contour plot of the function $\beta_{2c}=\beta_{2c}(\xi,\varepsilon_e)$.

$$R_t(\xi,\varepsilon_e) = f_{ct} b \beta_{1t}\left(1-\xi, \varepsilon_e \frac{\xi-1}{\xi}\right)\cdot(H-\xi H) \qquad (7b)$$

It is easy to solve equation (6) by try-and-error, as functions β_{1c} and β_{1t} are known. It can be solved n times, if n is the number of points believed sufficient to describe the moment-curvature diagram to be constructed. In order to achieve the j-th point, by as-

signing a certain value ξ_j of the adimensional neutral axis with $\xi_j \geq \xi_u$, ε_{ej} is then found by solving equation (6) and, for the linear strain distribution, $\varepsilon_{ij}=\varepsilon_{ej}\cdot(\xi_j-1)/\xi_j$ is also known. A j-th value $1/r_j=\theta_j$ of the curvature is then found, and has to be coupled with a j-th value M_j of the bending moment.

The solution is further easier for $\xi_j>1$, as R_{ct} becomes null and $\beta_{1c}=P/(0.85 f_c b \xi_j H)$ is immediately found from (6), so that ε_{ej} is then obtained from (4a).

Since from (6) ε_{ej}, as well as ε_{ij}, are now available for the assigned $\xi_j \geq \xi_u$, M_j is then found from the moment equilibrium. Say $R_{cj}=R_c(\xi_j,\varepsilon_{ej})$ and $R_{tj}=R_t(\xi_j,\varepsilon_{ij})$ the compressive and the tensile stress resultants obtained from (7a) and (7b), respectively, and say $d_{cj}(\xi_j,\varepsilon_{ej})=H/2-\beta_{2c}(\xi_j,\varepsilon_{ej})\xi_j H$ and $d_{tj}(\xi_j,\varepsilon_{ij})=H/2-\beta_{2c}(1-\xi_j,\varepsilon_{ij})\cdot(H-\xi_j H)$ their distance from the section centroid. Therefore M_j is:

$$M_j = R_{cj}(\xi_j,\varepsilon_{ej}) d_{cj}(\xi_j,\varepsilon_{ej}) + R_{tj}(\xi_j,\varepsilon_{ij}) d_{tj}(\xi_j,\varepsilon_{ij}) \quad (8)$$

with $R_{tj}=0$ for $\xi_j \geq 1$.

By achieving n points (θ_j, M_j) and plotting them in the plane defined by the reference system $(O; \theta, M)$, the moment-curvature diagram is finally found.

3.2 *Example of construction of a moment-curvature diagram to use the Model Column Method*

The above simple way of achieving moment-curvature diagrams allows us to easily analyze the column stability through the Model Column Method. The method is well known, and its application to the problem of this article is shown.

Consider a column made for instance of a sedimentary conglomerate. Its compressive and tensile strength are f_c=35 MPa and f_{ct}=3 MPa respectively, and Young's modulus is $E_c=3\cdot10^4$ MPa. The length of the column is for instance L=2 m, its cross section 24x24 cm^2, and it is fixed at its base. The vertical load at the top is P=1250 kN. For $P=N_u(\xi_u)$, the ultimate section strength is reached for ξ_u=0.951 with the ultimate moment $M_u(\xi_u)$=35905 Nm, corresponding to a curvature $\theta_u=12.81\cdot10^{-3}$ m^{-1}.

Due to column instability, both M_u and θ_u cannot be reached, as already for $\theta'=8.61\cdot10^{-3}$ m^{-1} the column loses its stability with a total moment M'_{I-II}=30000 Nm at its base, sum of the first order constant moment $M_I=Pe$=12550 Nm and of the contribute of the second order moment $M'_{II}=4(L^2/\pi^2)P\theta'$=17450 Nm. The latter, linearly depending on the curvature θ at the column base, reaches the above value proportional to the curvature $\theta'<\theta_u$.

The moment-curvature diagram of Figure 5 is constructed with 11 points, including the origin (0,0) for j=1 and the ultimate strength point (θ_u, M_u) for j=11. After the ultimate point with $\xi_{11}=\xi_u$=0.951, the previous 3 points (θ_j, M_j), for j=8,9,10 have been found for 3 different given values of ξ_j with $\xi_u \leqslant \xi_j < 1$, while, for $1<j<8$, the remainders have been found for $1 \leqslant \xi_j$.

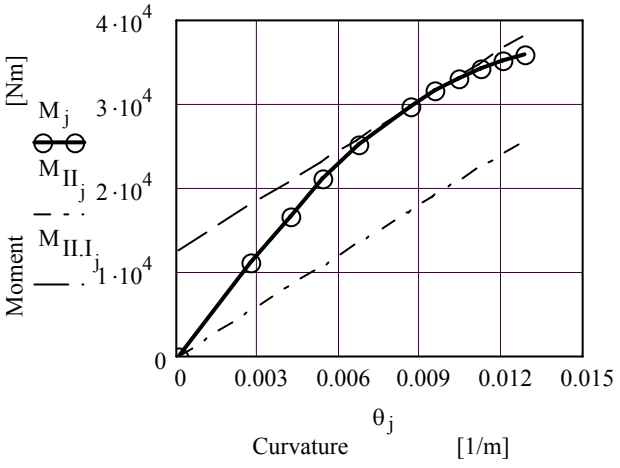

Figure 5. Moment-curvature diagram for P=1250 kN.

For instance the 9-th point has been found by assigning ξ_9=0.980 and by then solving (6) to find the unknown compressive strain $\varepsilon_{e9}=2.64\cdot10^{-3}$ and, consequently, the tensile strain ε_{i9} whose absolute value is $5.4\cdot10^{-5}$; $\theta_9=11.22\cdot10^{-3}$ m^{-1} is then found and, from (8), also M_9=34080 Nm. The 4-th point has been found by assigning ξ_4=1.3. Since R_t is null, from (6) we obtain $\beta_{1c}=P/(0.85 f_c b \xi_4 H)$=0.730 and, from (4a), $\varepsilon_{e4}=1.67\cdot10^{-3}$, as well as the compressive strain on the opposite edge $\varepsilon_{i4}=3.87\cdot10^{-4}$ and the curvature $\theta_4=5.37\cdot10^{-3}$ m^{-1}; from (8), also M_4=20990 Nm is finally found.

After having constructed the moment-curvature diagram, an advantage of the Model Column Method is that it can be graphically performed, both handwriting and with the computer aid.

It is worth making a further example. Suppose another fixed column made of the same quasi-brittle material, and with the same cross section. Its length is L=2.75 m, and the vertical load is P=500 kN. Therefore, at ultimate $N_u(\xi_u)=P$, with ξ_u=0.845, and $M_u(\xi_u)$=27620 Nm. By following the above procedure, the moment-curvature diagram is easily achieved (Fig. 6). It shows less section ductility with respect to the previous case with higher P: the moment-curvature diagrams show that the higher P, the higher the section ductility, as higher compressions allow higher plastic strains to develop. The curvature at ultimate is $\theta_u=4.08\cdot10^{-3}$ m^{-1}.

Contrarily to the previous example, in this case the second order moment, linearly depending on curvature θ, can reach the value $M_{II}=4(L^2/\pi^2)P\theta_u$, as $\theta_u=\theta'$ is reached without the column losing its stability before. Therefore, the total moment at ultimate is then $M_{I-II}=M_u$=27620 Nm, sum of the moments of second order M_{II}=6160 Nm and first order $M_I=Pe$=21460 Nm with e=4.3 cm.

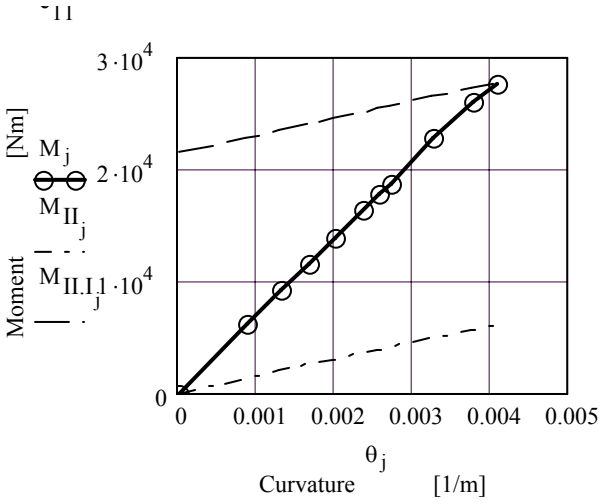

Figure 6. Moment-curvature diagram for P=500 kN.

4 FRACTURE STABILITY

The stability of the quasi-brittle notched column depends not only on its geometric stability, that is on the column slenderness and the elasto-plastic behaviour of the quasi-brittle material, but also on fracture stability, that also contributes to the whole stability of the column.

Fracture stability of quasi-brittle materials is in general investigated through models that in some way can take into account their cohesive fracture behaviour. Particularly, in some way they must be capable of describing the effects due to the fracture process zone extending over the tension softening region ahead of the traction-free crack.

In the Introduction we have shown that suitable models are for instance the Fictitious Crack Model and the Crack Band Model.

They are suitable in order to evaluate the fracture stability of the notched column: unfortunately, a Finite Element Model is usually necessary. The above models and algorithms are not always easily available for all engineers, unless they are specialized structural engineers, but often the stability of a stone column is evaluated by a building engineer or an engineer not suitably graduate to use these algorithms

Besides, usually a more intuitive approach is achieved without using the Finite Element Method, whose implementation is often rather complicate. Also, Finite Element Codes including the routine for the analysis of fracture stability are usually rather costly. Therefore, a simplified method of evaluating the fracture stability of the notched column is useful, both because more intuitive and because easy to be used, with almost no cost.

A suitable use of *R*-curves, or resistance curves, is then proposed, as it allows us an easy analysis of fracture stability, although approximate.

This approximate approach allows us to adapt the Linear Elastic Fracture Mechanics to the fracture behaviour of the quasi-brittle materials without using any "cohesive crack model", like the ones already quoted above.

R-curves can be obtained through the so–called "effective crack models" by taking into account the nonlinear fracture behaviour of a quasi-brittle material in an approximate manner. This approach allows us to perform fracture analysis of a real structure made of quasi-brittle material through an equivalent elastic structure containing an effective crack suitably longer than that of the real structure (Karihaloo 1995).

Two well known "effective crack models" are the Two-Parameter Model proposed by Jenq & Shah (1985) and the Effective Crack Model proposed by Nallathambi & Karihaloo (1986). These models allow us to construct *R*-curves, obtained by specific tests made on three or four point notched beams, the former by a CMOD versus load diagram by evaluating the compliance after unloading close to the peak load, the latter by deflection versus load diagrams obtained for different notch lengths plotted up to the peak load and by suitably comparing tangent and secant modulus in the different cases.

R-curves are also obtained as a an application of the Size Effect Model. Size effect on concrete was first studied by Bazant in 1976. Many studies have been made on intrinsic brittlness of concrete and on the size effect whose quasi-brittle materials are affected. In this paper it is sufficient to report that good brittleness indicators are the energy brittleness number proposed by Carpinteri (1982, 1986) and the structural brittleness number proposed by Bazant & Pfeiffer (1987).

Bazant studies on the size effect on concretes leaded to the following scaling law:

$$(\sigma_N)_u = \frac{B_0 f_{ct}}{\sqrt{1 + H / d_0}} \tag{9}$$

with:

$$B_0 = \frac{1}{f_{ct}} \left(\frac{E_c G_f}{g'(\alpha_0) c_f} \right)^{\frac{1}{2}} \qquad d_0 = c_f \frac{g'(\alpha_0)}{g(\alpha_0)} \tag{10}$$

where $\alpha_0 = a_0/H$ is the ratio between the crack length a_0 of the pre-cracked beam and its depth H, c_f and G_f. are the length of the fracture process zone and the energy required for crack growth, respectively, for an infinitely large specimen, namely for $H \to +\infty$, $g(\alpha_0)$ is the value calculated in α_0 of function g that, in general, depends, besides the scaling law, on the geometry function F referred to the specific geometry of pre-cracked specimens whose linear elastic

fracture behaviour is well known from laboratory tests. Of course, for the above definition, c_f and G_f are material properties. The former is strictly correlated with the structural brittleness number $1/\beta$ of Bazant & Pfeiffer already quoted above, with $\beta=H/d_0$. The latter is the asymptotic value of the fracture energy for infinitely large quasi-brittle specimens.

From the scaling law (9), Bazant's Size Effect Model allows us to derive *R*-curves in parametric form according to Bazant & Kazemi (1990).

It is first necessary to obtain function $g(\alpha)$, where α is the adimensional value a/H of a generic crack length a. This can be done by equating the square expression of the stress intensity factor as a function of α, obtained through the scaling law, to that obtained by Linear Elastic Fracture Mechanics for a four point beam subjected to not only bending but also compression.

Since the distance between the notch and the column top is practically equal to the length L of the column (Fig. 1), that is supposed to be notched in a region very close to its base, there the total bending moment is then $P(e+\Delta)$, where $\Delta = 4\theta' L^2/\pi^2$ is the second order eccentricity, the normal force is P, and there is no shear force. By neglecting the variation of the second order moment along the column, the stress and displacement field in the vicinity of the crack tip can be practically considered of pure mode I. Of course this is a simplification, as if the variation of the second order moment is not neglected, in this region shear is also present, the deformation at the crack tip is not of pure mode I, and this affects the direction of the crack growth. Nevertheless, since in this paper a simplified analysis is run, a further approximation of the method is that also the effects of deformation modes at the crack tip different from mode I are considered negligible.

The critical value of the stress intensity factor is then K_{Ic}, and for Bazant's scaling law it must be:

$$K_{Ic}(\alpha)^2 = \frac{P^2}{H^2 b^2} H\, g(\alpha) \tag{11}$$

while, for Linear Elastic Fracture Mechanics, it is:

$$K_{Ic}(\alpha)^2 = \frac{P^2}{H^2 b^2} H\, \pi \alpha\, F(\alpha)^2 \tag{12}$$

Since in the expression (12) K_{Ic} is obtained through Linear Elastic Fracture Mechanics, the *K*-superposition principle is allowed. Then, in the above expression (12), K_{Ic} is considered as the sum of K_{IcM}, related to a pure moment $M = P(e+\Delta)$ at the column base, and K_{IcN}, related to a uniform compression with resultant P.

In this latter expression $F(\alpha)=[6\eta_t F_M(\alpha) - F_N(\alpha)]$ is a geometry function with the contribute of both a term $F_M(\alpha)$ due to bending and a term $F_N(\alpha)$ due to uniform compression, and where $\eta_t=e_t/H$ is the adimensional total eccentricity, comprehensive also of the contribute of the second order displacement of the point of application of P with respect to the column base. The geometry functions $F_M(\alpha)$ and $F_N(\alpha)$ are easily available in the specialist literature (Tada et al. 2000), where $F_N(\alpha)$ is of course referred to single edge notched members with uniform tension: in the case analyzed in this paper, a negative sign before $F_N(\alpha)$ is then required.

$F_M(\alpha)$ is referred to the pure bending specimen, for instance a four points beam notched at mid-span where the moment M is constant; although in this case the moment along the column is not exactly constant due to the second order displacements, nevertheless close to the column base M is assumed to be almost constant and equal to Pe_t. The series development of $F_M(\alpha)$ is $F_M(\alpha) = 1.122 - +1.4\alpha+7.33\alpha^2-13.08\alpha^3+14.0\alpha^4$.

$F_N(\alpha)$ is instead referred to the single edge notched specimen subjected to constant normal tensile stress, so that its series development is: $F_N(\alpha) = 1.122-0.231\alpha+10.55\alpha^2-21.71\alpha^3+30.382\alpha^4$. In this case, the normal stress is assumed to be an uniform compressive stress $P/(bH)$, so that the contribute of $F_N(\alpha)$ to $F(\alpha)$ has negative sign.

By equating (11) to (12) $g(\alpha)$ is found, that is:

$$g(\alpha) = \pi \alpha F(\alpha) \tag{13}$$

Having evaluated the adimensional number $\beta=H/d_0$, if $\beta>0$, the parametric form of a *R*-curve can be obtained through the Size Effect Model, that is:

$$\Delta a(\alpha) = c_f \frac{g'(\alpha_0)}{g(\alpha_0)}\left[\frac{g(\alpha)}{g'(\alpha)} - (\alpha - \alpha_0)\right] \tag{14a}$$

$$R(\alpha) = G_f \frac{g'(\alpha)}{g'(\alpha_0)} \frac{\Delta a(\alpha)}{c_f} \tag{14b}$$

For a given compression force $P=N(\xi_u)$ with a certain total eccentricity e_t, the limit condition of stability of an edge notch with length a_0 at the column base can now be evaluated through the *R*–curve. The tensile stress that could make the fracture propagate is:

$$\sigma = \frac{6Pe_t}{bH^2} - \frac{P}{bH} \tag{15}$$

Therefore, besides the *R*-curve, also the energy release rate $\mathcal{G}$ can be defined in a parametric form through the parameter α, that is:

$$s(\alpha) = (\alpha - \alpha_0)H \tag{16a}$$

$$\mathcal{G}(\alpha)=\frac{\sigma^2\pi H}{E_c}\alpha \qquad (16b)$$

In the plane defined by the reference axis Δa and $\mathcal{G}$, by varying α the energy release rate $\mathcal{G}$ is a line starting from the point $-a_0$ on the abscissa axis, with positive first derivative, and that can intersect or not the *R*-curve. If the *R*-curve is intersected, the notch – with length a_0 and located at the base of the quasi-brittle column loaded by the force *P* applied with eccentricity *e* at the top and with total eccentricity e_t at the base – is stable. Contrarily, if the above line remains always above the *R*-curve without intersecting it, then fracture propagates from the notch with length a_0 catastrophically. Of course, the fracture instability limit state is reached when the line starting from the point $(-a_0,0)$ on the abscissa axis is tangent to the *R*-curve (Fig. 7). The abscissa Δa of the tangent point represents the amount of stable crack growth due to the application at the column top of the force *P* with eccentricity *e*.

The above parametric form of the *R*-curve makes it start for $\Delta a=0$; it then reaches its maximum value G_f for $\Delta a=c_f$, so that the smaller c_f, the higher the derivative of the *R*-curve, that then tends to infinity the more brittle the column is.

This method can be used only if c_f and G_f are known. They are evaluated by extrapolating them from the results of a certain number of four point tests of notched beams. Nevertheless, for very diffused stones, like for instance Carrara marble, Buddusò granite, Firenzuola sandstone (the so–called "pietra serena"), Absolute Black granite from Zimbabwe and so on, especially if sufficiently uniform, it would be desirable that not only their strength and Young's modulus can be found in some manuals, but also c_f and G_f. Besides, this could also happen for High Performance Concretes, with the diffusion of standard productions of specialist farms.

Having achieved c_f and G_f, the application of the method is easy. Consider the same quasi-brittle material of the examples of Paragraph 3.2, that, besides

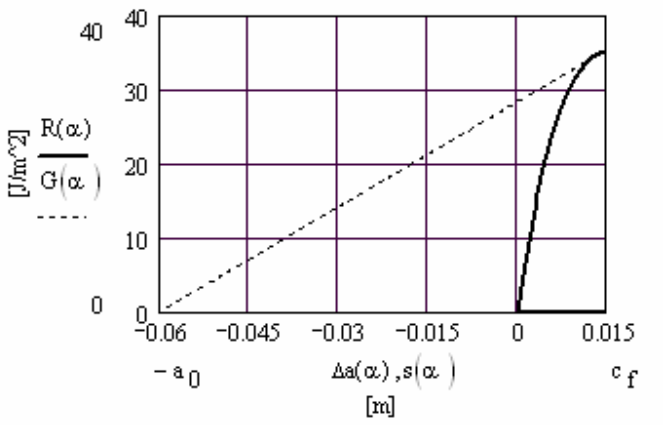

Figure 7. *R*-curve for α_0=0.25 with the line of the energy release rate $\mathcal{G}$ tangent to it.

the already quoted mechanical characteristics, has G_f=35 J/m^2 and c_f=15 mm.

Consider both examples of Paragraph 3.2, and assume that both columns are edge notched at their base with a_0=6 cm, so that α_0=0.25. The stability of columns with different length has to be evaluated, all with the same cross section of 24x24 cm^2.

The column 2.75 m long, if not damaged, for P=500 kN could reach the resistant moment M_u=27620 Nm for ξ_u=0.845 and $\theta_u=4.08\cdot10^{-3}$ m^{-1} without losing its stability before; if notched, for instance with α_0=0.25, the interaction diagram is then restrained by fracture instability.

Actually, in this case from the *R*–curve of Figure 7 drawn for α_0=0.25, we find that fracture propagates catastrophically already for e=3.74 cm and first order moment Pe=18700 Nm. By also including the second order moment M'_{II}=6166 Nm due to the second order eccentricity of 1.23 cm, a total moment $M'_{I-II}=M'_I+M'_{II}$=24850 Nm is obtained, lower than M_u=27620 Nm. This is shown in Figure 8 where, for P=500 kN, this total moment lies on the dashed curve restraining the interaction diagram for α_0=0.25. This dashed curve is drawn for every total moment $M'_{I-II}=M'_I+M'_{II}$ for different values of *P* till it intersects the interaction diagram on its right side and, on its left side, the ordinate axis at the point representative of pure bending of a notched beam.

Of course M'_{I-II} is not in general among the design data, while usually the designer knows the original eccentricity *e* of the vertical load, so that what is known is $M'_I=Pe$. From the *R*-curve, drawn in Figure 7 through equations (14) for α_0=0.25, it can be found the limit value of *e* that cannot be overcome for P=500 kN in order to avoid the collapse due to a catastrophic fracture propagation. The line defining the energy release rate $\mathcal{G}$ starting from the point with coordinates (–0.06 m, 0) on the abscissa axis is then drawn, and has to be tangent to the *R*-curve. This is the limit condition of fracture growth arrest at the column base when *P* is applied with eccentricity *e* at the column top.

Since from the moment-curvature diagram we know that the second order eccentricity at the column base is $\Delta=4(L^2/\pi^2)\theta_u$=1.23 cm for $\theta_u=4.08\cdot10^{-3}$ m^{-1}, then the line $\mathcal{G}$ is tangent to the *R*-curve if the tensile stress $\sigma=6P(e+\Delta)/(bH^2)-P/(bH)$ at the edge in tension does not overcome 2.11 MPa. With such a value of σ due to the total moment, the stable fracture growth with Δa=12.5 mm occurs for $\mathcal{G}$=34.3 J/m^2. This happens for *e* not higher than 3.74 cm with $M'_I=Pe$=18700 Nm: in Figure 8 this moment lies on the solid curve for α_0=0.25, and its ordinate difference from the dashed curve of total moments allowed by fracture stability is the second order moment $M'_{II}=P\,\Delta$=6150 Nm. For α_0=0.25 the solid curve intersects the ordinate axis in a point representing pure bending of a notched beam with α_0=0.25 that collapses with moment of 5000 Nm.

On its right region, this solid curve, together with the others with different notch length, merges into a unique curve that restrains the interaction diagram due to only geometric instability.

These right parts of the solid curves restraining the interaction diagram for only geometric instability are now investigated through the other example of Paragraph 3.2. For P=1250 kN, the other column 2 m long could reach the resistant moment M_u=35905 Nm for ξ_u=0.951 and θ_u=12.81·10^{-3} m^{-1}, but the geometrical instability restrains it to M'_{I-II}=30000 Nm, sum of M_I=Pe=12550 Nm and M'_{II}=17450 Nm, and achieved for θ'=8.62·10^{-3} m^{-1}<θ_u and with ξ'=1.06>ξ_u. In Figure 8 it is shown that, for P=1250 kN, the total moment M'_{I-II}=30000 Nm lies on the dashed curve that, for the length L=2 m representing the column slenderness, restrains the interaction diagram M-N, and that is described by different total moments M'_{I-II}=M'_I+M'_{II} for different values of P. Of course, in general M'_{I-II} is not among the design data, while usually what is known is M'_I=Pe. For P=1250 kN, the maximum allowed value of e is 1 cm, and Pe=12550 Nm lies on the solid curve with L=2 m. This solid curve determined by only geometric instability actually restrains the interaction diagram for the designer. Contrarily, for P=1250 kN and α_0=0.25 fracture does not propagate and does not restrain the interaction diagram, as seen in Figure 8. By using the R–curve drawn for α_0=0.25, we actually find that fracture is stable till e=3.02 cm and moment Pe=37750 Nm. By also including the second order moment M'_{II}=17450 Nm due to the second order eccentricity Δ=4(L^2/π^2)θ'=1.4 cm at the base, we would obtain a total moment of 55200 Nm, that is much higher than M_u=35905 Nm. However, having first reached the section ultimate strength for P=1250 kN, the column would collapse before fracture propagation.

Figure 8 shows that for P=1250 kN neither with

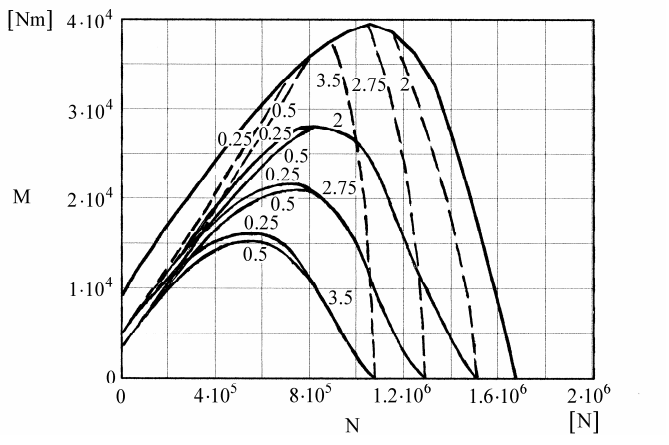

Figure 8. Interaction diagram restrained by both geometric and fracture instability.

α_0=0.5 fracture stability restrains the N-M diagram.

5 CONCLUSIONS

A simplified analysis of the stability of a column made of quasi-brittle material, edge notched at its base and eccentrically loaded at the top by a vertical force is described. It is worth studying simple check methods because, otherwise, this problem can only be studied through finite elements, due to different nonlinearities: the geometric one, that of the mechanical behaviour of the material, as well as the one of the fracture behaviour of quasi-brittle materials. Simplified methods have been used: the Model Column Method, to analyze geometric instability, and used after obtaining the moment-curvature diagrams with a simplified method, and the R-curves, obtained through the Size Effect Model of the fracture behaviour of quasi-brittle materials, to analyze fracture instability. By opportunely coupling these methods, we have been able to restrain the column interaction diagram with curves that take into account both fracture and geometric instability for different column slenderness and notch length.

Through this simple analysis performed with few calculations, it is shown that, for low values of the vertical load, fracture instability, by also taking into account the second order moments, actually restrains the interaction diagram, the more the lower the vertical load. Contrarily, for higher values of the vertical load, fracture cannot propagate catastrophically, as tensile stresses in the region close to the notch are not high enough due to the high compression force, unless also eccentricity becomes high enough. In this latter case the ultimate strength of the section is reached before fracture propagation. Therefore, in this case, with high vertical loads, the interaction diagram is only restrained by geometric instability.

ACKNOWLEDGEMENTS

The study refers to a research project on the advanced structural use of stone in architecture and building engineering, supported by the Sardegna Ricerche Consortium, managed by the PROMEA Consortium, and run by the Department of Structural Engineering with the Department of Mechanical Engineering of the University of Cagliari.

The author is very grateful to Professor Luigi Cedolin, Chair of Structural Analysis and Design, Politecnico di Milano, for having kindly read an extended abstract of this paper, and given his valuables suggestions.

Special thanks go to Professor Pietro Gambarova, Chair of Structural Analysis and Design, Politecnico di Milano, for his valuable advises and encouragements in carrying out this study after a critical reading of the extended abstract of this paper.

REFERENCES

Bazant, Z.P. 1976. Instability, ductility and size effect in strain-softening concrete, *ASCE J Eng Mech,* 102, 331-344.

Bazant, Z.P. 1984. Size effect in blunt fracture: concrete, rock, metal, *ASCE J Eng Mech,* 110, 518-535.

Bazant, Z.P. 1987. Fracture energy of heterogeneous materials and similitude, In *G-28*, 229-241.

Bazant, Z.P. & Cedolin, L. 1979. Blunt crack band propagation in finite element analysis, *ASCE J Eng Mech,* 105, 297-315.

Bazant, Z.P. & Cedolin, L. 1991. *Stability of structures*. e*lastic, inelastic, fracture, and damage theories*. New York: Oxford University Press.

Bazant, Z.P. & Kazemi, M.T. 1990. Determination of fracture energy, process-zone length and brittleness number from size effect, with application to rock and concrete, *Int J Fracture*, 44, 111-131.

Bazant, Z.P. & Oh, L. 1983. Crack band theory for fracture of concrete, *Mater Struct,* 16, 155-157.

Bazant, Z.P. & Pfeiffer, P.A. 1987. Determination of fracture energy properties from size effect and brittleness number, *ACI Mater J*, 84, 463-480.

Biasioli, F., Debernardi, P.G. & Marro, P. 1993. *Eurocodice 2. Esempi di calcolo.* Turin: Edizioni Keope Srl.

Carpinteri, A. 1982. Notch sensitivity in fracture testing of aggregative materials, *J Eng Fracture Mech*, 16, 467-481.

Carpinteri, A. 1986. *Mechanical damage and crack growth in concrete: plastic collapse to brittle fracture*. Dordrecht: Martinus Nijhoff Publishers.

Hillerborg, A., Modéer, M. & Petersson, P.E. 1976. Analysis of crack formation and crack growth in concrete by means of fracture mechanics and finite elements, *Cement Concr Res*, 6, 773-782.

Jenq, Y.S. & Shah, S.P. 1985. A two-parameter fracture model for concrete, *ASCE J Eng Mech,* 111, 1227-1241.

Karihaloo, B.L. 1995. Fracture Mechanics and structural concrete. Burnt Mills (UK) Longman Scientific & Technical

Nallathambi, P. & Karihaloo, B.L. 1986a. Determination of the specimen-size independent fracture toughness of plain concrete, *Mag Concr Res*, 38, 67-76.

Nallathambi, P. & Karihaloo, B.L. 1986b. Prediction of load deflection behaviour of plain concrete based on fracture energy, *Cement Concr Res*, 16, 373-382.

Sargin, M. 1971. Stress strain relationships for concrete and the analysis of structural concrete sections, Dept. of Civil Eng., University of Waterloo, Solid Mechanics Division, S.M. Study No.4.

Tada, H., Paris, P.C. & Irwin, G.R. 2000. *The Stress Analysis of Cracks Handbook*. New York: ASME Press.